



# Fast and Flexible Software Polar List Decoders

Mathieu Léonardon<sup>1,2</sup>  · Adrien Cassagne<sup>1,3</sup> · Camille Leroux<sup>1</sup> · Christophe Jégo<sup>1</sup> · Louis-Philippe Hamelin<sup>4</sup> · Yvon Savaria<sup>2</sup>

Received: 13 October 2017 / Revised: 25 July 2018 / Accepted: 11 December 2018 / Published online: 18 January 2019  
© Springer Science+Business Media, LLC, part of Springer Nature 2019

## Abstract

Flexibility is one mandatory aspect of channel coding in modern wireless communication systems. Among other things, the channel decoder has to support several code lengths and code rates. This need for flexibility applies to polar codes that are considered for control channels in the future 5G standard. This paper presents a new generic and flexible implementation of a software Successive Cancellation List (SCL) decoder. A large set of parameters can be fine-tuned dynamically without re-compiling the software source code: the code length, the code rate, the frozen bits set, the puncturing patterns, the cyclic redundancy check, the list size, the type of decoding algorithm, the tree-pruning strategy and the data quantization. This generic and flexible SCL decoder enables to explore tradeoffs between throughput, latency and decoding performance. Several optimizations are proposed to achieve a competitive decoding speed despite the constraints induced by the genericity and the flexibility. The resulting polar list decoder is about 4 times faster than previous generic software decoders and only 2 times slower than previous non-flexible unrolled decoders. Thanks to the flexibility of the decoder, the fully adaptive SCL algorithm can be easily implemented and achieves higher throughput than any other similar decoder in the literature, up to 425 Mb/s on a single processor core for  $N = 2048$  and  $K = 1723$  at 4.5 dB.

**Keywords** Polar codes · Adaptive successive cancellation list decoder · Software implementation · 5G standard · Generic decoder · Flexible decoder

## 1 Introduction

Polar codes [1] are the first provably capacity achieving channel codes, for an infinite code length. The decoding performance of the original Successive Cancellation (SC) decoding algorithm is however not satisfactory for short polar codes. The Successive Cancellation List (SCL) decoding algorithm has been proposed in [2] to counter this fact along with the concatenation of a Cyclic Redundancy Check (CRC). The decoding performance of SCL decoding is such that polar codes are included in the fifth generation (5G) mobile communications standard [3].

Cloud radio access network (Cloud-RAN) is foreseen by both academic [4, 5] and industrial [6, 7] actors as one of the key technologies of the 5G standard. In Cloud-RAN the

virtualization of the physical layer (PHY) would allow for deep cooperative multipoint processing and computational diversity [4]. PHY-layer cooperation enables interference mitigation, while computational diversity lets the network balance the computational load across multiple users. But the virtualization of the FEC decoder is a challenge as it is one of the most computationally intensive tasks of the signal processing chain in a Cloud-RAN context [8, 9]. Therefore, efficient, flexible and parallel software implementations of FEC decoders are needed to enable some of the expected features of Cloud-RAN.

To date, the fastest software implementations of SCL polar decoders have been proposed in [10]. The high decoding speed is achieved at the price of flexibility, because the software decoder is only dedicated to a specific polar code. In a wireless communication context, the source code of this fast software polar decoder would have to be recompiled every time the Modulation and Coding Scheme (MCS) changes, which may happen every millisecond.

In this work, we propose a software SCL polar decoder able to switch between different channel coding contexts

---

✉ Mathieu Léonardon  
mathieu.leonardon@u-bordeaux.fr

(block length, code rate, frozen bits sets, puncturing patterns and CRC code). This property is denoted as *genericity*. Moreover, the proposed decoder supports different list-based decoding algorithms, several list sizes ( $L$ ), quantization formats and tree-pruning techniques during a real time execution. Again, this is done dynamically without having to recompile the software description. We denote this feature as *flexibility*. The genericity and the flexibility of the decoder are achieved without sacrificing the decoding throughput and latency thanks to several implementation optimizations. Actually, the proposed software SCL decoder is only 2 times slower than a polar code specific decoder [10] and 4 times faster than a generic decoder [11]. The adaptive version of the decoder reaches 425 Mb/s on a single processor core for  $N = 2048$ ,  $K = 1723$  and  $L = 32$  at 4.5 dB.

This paper includes several contributions. The most significant of them are listed in this paragraph. i) Unlike previously proposed decoders, the proposed software decoder uses quantized information. ii) Two different partial sum management methods are presented and their advantages and weaknesses are discussed. iii) Novel methods to speed up the CRC processing are presented that greatly improve the throughput of adaptive versions of the decoding algorithms. iv) A sorting technique [12] particularly suited for software implementations further increases the decoding throughput. v) Unlike previous comparable implementations, the proposed decoder also supports a fully adaptive version of SCL. Thanks to these improvements, the exploration of polar coding and decoding is greatly facilitated : many computationally intensive configurations are explored, and their error rate is reported down to very low error rates. vi) Finally, in a previous work, the use of a specific kind of tree pruning was presented as severely degrading the error correction performance in most cases. In this paper, it is shown that in many cases, the degradation is very low while the throughput gains are significant.

The rest of the paper is organized as follows: Section 2 describes the SCL decoding algorithm and its variants. The genericity and the flexibility of the proposed decoder are highlighted in Section 3. Section 4 details the speed-oriented optimizations. Finally, Section 5 reports the obtained throughput and latency performances.

## 2 Polar Codes

In this section, the polar encoding process is first presented, then the SC and SC-List based decoding algorithms are

reviewed. Finally, the tradeoffs between speed and decoding performance of different decoding algorithms are discussed.

### 2.1 Polar Encoding Process

In the polar encoding process, an information sequence  $\mathbf{b}$  of length  $K$  is transformed into a codeword  $\mathbf{x}$  of length  $N$ . The first step is to build a vector  $\mathbf{u}$  in which the information bits  $\mathbf{b}$  are mapped on a subset  $\mathbf{u}_{\mathcal{A}}$  where  $\mathcal{A} \subset \{0, \dots, N-1\}$ . The remaining bits  $\mathbf{u}_{\mathcal{A}^c} = (a_i : i \notin \mathcal{A})$  called *frozen bits* are usually set to zero. The selection of the frozen bits is critical for the effectiveness of the polar codes. Two of the main techniques to date for constructing polar codes are based on the Density Evolution approach [13] and on the Gaussian Approximation [14]. In this paper, all the evaluated polar codes were generated with the Gaussian Approximation method. These techniques sort the polar channels according to their reliability in order to choose the frozen bits set for a given code length. Then, an intermediate vector  $\mathbf{u}'$  is generated thanks to an encoding matrix:<sup>1</sup>  $\mathbf{u}' = \mathbf{u}F^{\otimes n}$ . Finally the bits in the subset  $\mathbf{u}'_{\mathcal{A}^c}$  are set to zero and the output codeword is  $\mathbf{x} = \mathbf{u}'F^{\otimes n}$ . This encoding method is called systematic because the *information sequence*  $\mathbf{b}$  is present in the codeword ( $\mathbf{x}_{\mathcal{A}} = \mathbf{b}$ ). In this paper, only systematic encoding schemes are considered. A CRC of length  $c$  may be concatenated to the information sequence  $\mathbf{b}$  in order to improve the decoding performance of SCL decoding algorithms. In this case,  $|\mathcal{A}| = K + c$  and the CRC bits are included in  $\mathbf{u}_{\mathcal{A}}$ . In this paper, the code rate is defined as  $R = K/N$  and the  $c$  bits of the CRC are not considered as information bits. For instance, a polar code whose block length is  $N = 2048$  and code rate is  $R = 1/2$  contains 1024 informations bits. Such a code is denoted as (2048,1024).

### 2.2 Polar Decoding Algorithms

#### 2.2.1 SC Decoding Algorithm

The SC decoding process can be seen as the pre-order traversal of a binary tree as shown in Fig. 1. The tree contains  $\log_2 N + 1$  layers. Each layer contains  $2^d$  nodes, where  $d$  is the depth of the layer in the tree. Each node contains a set of  $2^{n-d}$  Log-Likelihood Ratios (LLRs)  $\lambda$  and partial sums  $\hat{s}$ . The partial sums correspond to the propagation towards the top of the tree of hard decisions

$${}^1F^{\otimes 1} = \begin{bmatrix} 1 & 0 \\ 1 & 1 \end{bmatrix} \text{ and } \forall n > 1, F^{\otimes n} = \begin{bmatrix} F^{\otimes n-1} & 0_{n-1} \\ F^{\otimes n-1} & F^{\otimes n-1} \end{bmatrix}, \text{ where } n = \log_2(N), N \text{ is the codeword length, and } 0_n \text{ is a } 2^n\text{-by-}2^n \text{ matrix of zeros.}$$

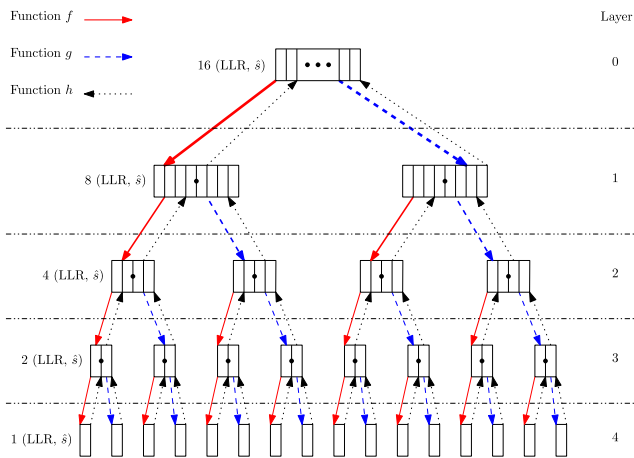


Figure 1 Full SC decoding tree ( $N = 16$ ).

made in the *update\_paths()* function. As shown in Fig. 1, LLRs, which take real values, and partial sums, which take binary values, are the two types of data contained in the decoding tree, and three functions, *f*, *g* and *h* are necessary for updating the nodes:

$$\begin{cases} f(\lambda_a, \lambda_b) &= \text{sign}(\lambda_a \cdot \lambda_b) \cdot \min(|\lambda_a|, |\lambda_b|) \\ g(\lambda_a, \lambda_b, \hat{s}_a) &= (1 - 2\hat{s}_a)\lambda_a + \lambda_b \\ h(\hat{s}_a, \hat{s}_b) &= (\hat{s}_a \oplus \hat{s}_b, \hat{s}_b) \end{cases}$$

In comparison with the SCL algorithm and its derivatives, the computational complexity of the SC algorithm is low:  $O(N \log_2 N)$ . Therefore, both software [15] and hardware [16] implementations achieve multi-Gb/s throughputs with low latencies. The drawback of the SC decoding algorithm is its decoding performance especially for short polar codes. This is an issue for the future 5G wireless standard in which polar codes are targeted for control channels, with code lengths shorter than 2048 [3].

### 2.2.2 SCL Decoding Algorithm

The SCL algorithm is summarized in Algorithm 1. Unlike the SC algorithm, the SCL decoder builds a list of candidate codewords along the decoding. At each call of the *update\_paths()* sub-routine (Alg. 1, 1.16),  $2L$  candidates are generated. A path metric is then evaluated to keep only the  $L$  best candidates among the  $2L$  paths. The path metrics are calculated as in [17]. At the end of the decoding process, the candidate codeword with the best path metric is selected in the *select\_best\_path()* sub-routine (Alg. 1, 1.18). The decoding complexity of the SCL algorithm grows as  $O(LN \log_2 N)$ . This linear increase in complexity with  $L$  comes with significant improvements of Bit Error Rate (BER) and Frame Error Rate (FER) performances, especially for small code lengths.

### Algorithm 1 SCL decoding algorithm

```

Data:  $\lambda$  is a 2D buffer ( $[L][2N]$ ) to store the LLRs.
Data:  $\hat{s}$  is a 2D buffer ( $[L][N]$ ) to store the bits.
1 Function SCL_decode ( $N, o_\lambda, o_s$ )
2    $N_{\frac{1}{2}} = N/2$ 
3   if  $N > 1$  then // not a leaf node
4     for  $p = 0$  to  $L - 1$  do // loop over the paths
5       for  $i = 0$  to  $N_{\frac{1}{2}} - 1$  do // apply the f function
6          $\lambda[p][o_\lambda + N + i] =$ 
7            $f(\lambda[p][o_\lambda + i], \lambda[p][o_\lambda + N_{\frac{1}{2}} + i])$ 
8         SCL_decode ( $N_{\frac{1}{2}}, o_\lambda + N, o_s$ )
9       for  $p = 0$  to  $L - 1$  do
10        for  $i = 0$  to  $N_{\frac{1}{2}} - 1$  do // apply the g function
11           $\lambda[p][o_\lambda + N + i] = g(\lambda[p][o_\lambda +$ 
12             $i], \lambda[p][o_\lambda + N_{\frac{1}{2}} + i], \hat{s}[p][o_s + i])$ 
13          SCL_decode ( $N_{\frac{1}{2}}, o_\lambda + N, o_s + N_{\frac{1}{2}}$ )
14        for  $p = 0$  to  $L - 1$  do
15          for  $i = 0$  to  $N_{\frac{1}{2}} - 1$  do // update the partial sums
16             $\hat{s}[p][o_s + i] =$ 
17               $h(\hat{s}[p][o_s + i], \hat{s}[p][o_s + N_{\frac{1}{2}} + i])$ 
18        else // a leaf node
19          update_paths () // update, create and delete paths
20   SCL_decode ( $N, 0, 0$ ) // launch the decoder
21   select_best_path ()

```

### 2.2.3 Simplified SC and SCL Decoding Algorithms

All aforementioned polar decoding algorithms have in common that they can be seen as a pre-order tree traversal algorithm. In [18], a tree pruning technique called the Simplified SC (SSC) was applied to SC decoding. An improved version was proposed in [16]. This technique relies on the fact that, depending on the frozen bits location in the leaves of the tree, the definition of dedicated nodes enables to prune the decoding tree: Rate-0 nodes (R0) correspond to a sub-tree whose all leaves are frozen bits, Rate-1 nodes (R1) correspond to a sub-tree in which all leaves are information bits, REPetition (REP) and Single Parity Check (SPC) nodes correspond to repetition and SPC codes sub-trees. These special nodes, originally defined for SC decoding, can be employed in the case of SCL decoding as long as some modifications are made in the path metric calculation [10]. This tree-pruned version of the algorithm is called Simplified SCL (SSCL). The tree pruning technique can drastically reduce the amount of computation in the decoding process. Moreover, it increases the available parallelism by replacing small nodes by larger ones. As will be discussed in Section 3, the tree pruning may have a small impact on decoding performance.

### 2.2.4 CRC Concatenation Scheme

The authors in [2] observed that when a decoding error occurs, the right codeword is often in the final list, but not with the best path metric. They proposed to concatenate a CRC to the codeword in order to discriminate the candidate codewords at the final stage of the SCL decoding. Indeed, this technique drastically improves the FER performance of the decoder. We denote this algorithm CA-SCL and its simplified version CA-SSCL. In terms of computational complexity, the overhead consists in the processing of  $L$  CRCs at the end of each decoding.

### 2.2.5 Adaptive SCL Decoding Algorithm

The presence of the CRC can be further used to reduce the decoding time by gradually increasing  $L$ . This variation of SCL is called Adaptive SCL (A-SCL) [19]. The first step of the A-SCL algorithm is to decode the received frame with the SC algorithm. Then, the decoded polar codeword is checked with a CRC. If the CRC is not valid, the SCL algorithm is applied with  $L = 2$ . If no candidate in the list satisfies the CRC,  $L$  is iteratively doubled until it reaches the value  $L_{max}$ . In this paper, we call this version of the A-SCL decoding the Fully Adaptive SCL (FA-SCL) as opposed to the Partially Adaptive SCL (PA-SCL), in which the  $L$  value is not iteratively doubled but directly increased from 1 (SC) to  $L_{max}$ . The simplified versions of these algorithms are denoted PA-SSCL and FA-SSCL. In order to simplify the algorithmic range, in the remainder of the paper, only the simplified versions are considered. The use of either FA-SSCL or PA-SSCL algorithmic improvement introduces no BER or FER performance degradation as long as the CRC length is adapted to the polar code length. If the CRC length is too short, the decoding performance may be degraded because of false detections. These adaptive versions of SSCL can achieve higher throughputs. Indeed, a large proportion of frames can be decoded with a single SC decoding. This is especially true when the SNR is high. This will be further discussed in Section 3.

## 2.3 Algorithmic Comparison

In order to better distinguish all the algorithmic variations, we compare their main features in Table 1. Each algorithm is characterized in terms of decoding performance, throughput, and worst case latency for a software implementation. The non-simplified versions of the adaptive SCL algorithms are not included in the Table 1 for readability.

The SC and especially the SSC algorithms achieve very high throughput and low latency with poor BER and FER performances. The SCL algorithm improves the

**Table 1** Throughput and latency comparison of polar decoding algorithms.

Decoding Algorithm	BER & FER Performances	Throughput ( $\mathcal{T}$ )	Max. Latency ( $\mathcal{L}_{worst}$ )
SC	poor	medium	medium
SSC	poor	high	low
SCL	good	low	high
SSCL	good	low	medium
CA-SSCL	very good	low	medium
PA-SSCL	very good	high	medium
FA-SSCL	very good	high	high

decoding performance compared to the SC algorithm, but its computational complexity leads to an increased latency and a lower throughput. The SSCL algorithm improves the decoding throughput and latency without any impact in terms of BER and FER performances, as long as the tree pruning is not too deep, as will be discussed in Section 3. Therefore, tree pruning is applied to all the following algorithms, namely CA-SSCL, FA-SSCL and PA-SSCL. By applying CRC to the SCL algorithm, one can achieve better BER and FER performances at the cost of computational complexity overhead. The Adaptive SCL algorithms reduce the decoding time with no impact on BER and FER performances as long as the CRC is carefully chosen. Furthermore, a tradeoff between throughput and worst case latency is possible with the use of either PA-SSCL or FA-SSCL decoding algorithms.

CA-SCL decoding performances for large code lengths ( $N > 2^{14}$ ) combined with large list sizes ( $L > 8$ ) are rarely reported in the literature. This is probably due to the long simulation time. The proposed decoders are integrated in the AFF3CT<sup>2</sup> toolset. Therefore, multi-threaded and multi-nodes simulations are enabled to handle such computation-demanding simulations.

All the presented simulations use the Monte Carlo method with a Binary Phase-Shift Keying (BPSK) modulation. The communication channel is an Additive White Gaussian Noise (AWGN) channel based on the Mersenne Twister pseudo-random number generator (MT19937) [20] and the Box-Muller transform [21]. Figure 2 compares the BER and FER performances of CA-SCL with SC decoding for a large range of code lengths. As expected, it appears that the coding gain brought by the SCL algorithm decreases for larger  $N$  values. In the case of  $N = 2^{16}$ , the improvement caused by the use of the CA-SCL algorithm with  $L = 32$

<sup>2</sup>AFF3CT is an Open-source software (MIT license) for fast forward error correction simulations, see <http://aff3ct.github.io>.

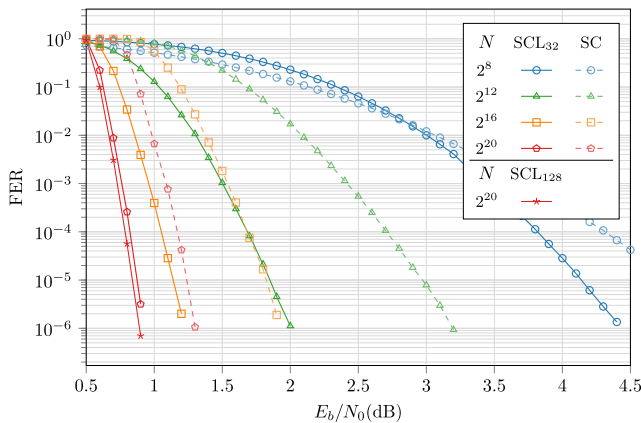


**Figure 2** Decoding performance comparison between CA-SCL and SC decoders. Code rate  $R = 1/2$ , and 32-bit CRC (GZip).

and a 32-bit GZip CRC (0x04C11DB7 polynomial) instead of SC is about 0.75 dB compared to 1.2 dB with a polar code of size  $N = 2^{12}$ . For larger polar codes,  $N = 2^{20}$ , the gain is reduced to 0.5 dB, even with a list depth of 128 that is very costly in terms of computational complexity.

The tradeoffs between speed and decoding performance show some general trends. However, the efficiency of each decoding algorithm is strongly dependent on the polar code length, code rate, list depth and code construction. It is expected that the best tradeoff is not always obtained with a single algorithm and parameter set combination. It is consequently highly relevant to use a generic and flexible decoder that supports all variants of the decoding algorithms. Thus, it is possible to switch from one to another as shown in the following section.

### 3 Generic and Flexible Polar Decoder

The main contribution of this work lies in the flexibility and the genericity of the proposed software decoder. These terms need to be clearly defined in order to circumvent possible ambiguity. In the remainder of the paper, the *genericity* of the decoder concerns all the parameters that define the supported polar code such as the codeword length, the code rate, the frozen bits set, the puncturing patterns and the concatenated CRC. These parameters are imposed by the telecommunication standard or the communication context. In the wireless communications context, these are constantly adapted by AMC methods [22]. In this work, a decoder is considered *generic* if it is able to support any combination of these parameters that can be changed during a real time execution. On the other hand, the *flexibility* of a decoder includes all the customizations that can be applied to the decoding algorithm for a given polar code such as

variants of the decoding algorithm, data quantization, list size  $L$ , tree pruning strategy. These customizations are not enforced by a standard. The flexibility gives some degrees of freedom to the decoder in order to find the best tradeoff between decoding performance, throughput or latency for a given polar code.

### 3.1 Genericity

In the context of wireless communications, the standards enforce several different code lengths  $N$  that have to be supported to share bandwidth between different users. This is also the case for the code rate  $R$  that needs to be adapted to the quality of the transmission channel. Therefore, a practical implementation should be adapted to both  $N$  and  $R$  in real-time in order to limit latency.

A polar code is completely defined by  $N$  and the frozen bits set  $u_{Ac}$ . Several methods exist to generate some "good" sets of frozen bits [13, 14]. The code rate  $R$  depends on the size of  $u_{Ac}$ . In their original form, polar code lengths are only powers of two. The puncturing and shortening techniques in [23–25] enable to construct polar codes of any length at the cost of slightly degraded decoding performance. The coding scheme can be completed with the specification of a CRC.

In [10], the unrolling method is used: a specific description of the decoder has to be generated for a specific polar code parameter set of  $N, K, R$ , frozen bits set, puncturing pattern, CRC. This approach leads to very fast software decoders at the price of the genericity, since a new source code should be generated and compiled every time the modulation and coding scheme (MCS) changes. This method is not adapted to wireless communication standards, in which these parameters have to be adapted not only over time, but also for the different users.

The proposed decoder does not use the unrolling method and is completely generic regarding the code dimension  $K$ , the code length  $N$ , the frozen bits set  $u_{Ac}$  and the puncturing patterns. All of them are dynamic parameters of the decoder and can be defined in input files. All CRC listed in [26] are available along with the possibility to define others. It is shown in [27] that custom CRCs for polar codes can have a significant impact on the decoding performance.

Relying on an unique software description implies that the tree pruning technique also has to be dynamically defined. Indeed, this technique depends on the frozen bits set  $u_{Ac}$ . Not sacrificing throughput or latency, while maintaining the genericity imposed by wireless communication standards, is at the core of the proposed implementation. Flexibility in terms of decoding algorithms, described in the following, along with improvements presented in Section 4, is necessary to deal with this challenge.

### 3.2 Flexibility

On one hand, the reason for the decoder genericity is the compliance to the telecommunication standards. On the other hand, the flexibility of the decoder regroups several algorithmic variations that are discussed in the following. These variations allow several tradeoffs of multiple sorts, irrespective of the standard. They are all included in a single source code.

In the proposed decoders the following parameters can be changed dynamically without re-compilation: the list size  $L$ , the tree pruning strategy, the quantization of the LLRs and the different SCL variants. Each of these adjustments can be applied to obtain different tradeoffs between throughput, latency, and error rate performance. As a consequence, one can easily fine-tune the configuration of the software decoder for any given polar code.

#### 3.2.1 List Size

As mentioned earlier, the list size  $L$  impacts both speed and decoding performance. In Fig. 3, the information throughput as well as BER and FER performances of the CA-SSCL algorithm are shown for different  $L$  values. A (2048,1024) polar code with a 32-bit CRC is considered. The computational complexity increases linearly with  $L$ : the throughput is approximately halved when  $L$  is doubled, except for the case of the SC algorithm ( $L = 1$ ) which is much faster. Indeed, there is no overhead due to the management of different candidate paths during the decoding. For  $L \geq 4$  and  $E_b/N_0 = 2$ , the FER is also approximately halved when the list size  $L$  is doubled.

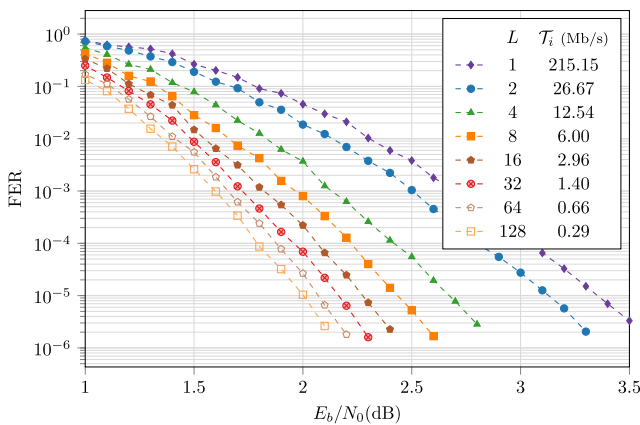


**Figure 3** Tradeoffs between CA-SSCL decoding and throughput performances depending on  $L$ .  $R = 0.5$ , and 32-bit CRC (GZip). For  $L = 1$ , the SSC decoder is used with a (2048,1024) polar code.

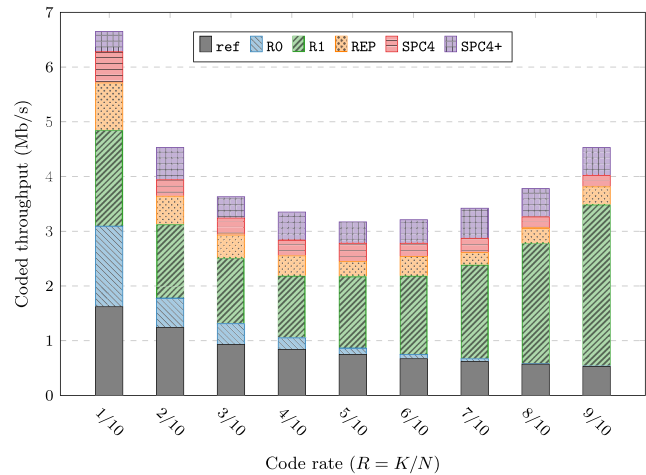


**Figure 4** Dedicated nodes impact, CA-SSCL.  $N = 2048$  and  $L = 32$ .

#### 3.2.2 Tree Pruning Strategy

A second degree of flexibility is the customization of the SCL tree pruning. The authors in [10, 18] defined dedicated nodes to prune the decoding tree and therefore to reduce the computational complexity. In the proposed decoders, each dedicated node can be activated separately. The ability to activate dedicated nodes at will is useful in order to explore the contribution of each node type on the throughput. Figure 4 shows the impact of the different tree pruning optimizations on the CA-SSCL decoder throughput depending on the code rate. The performance improvements are cumulative. Coded throughput, in which the redundant bits are taken in account, is shown instead of information throughput, for which only information bits are considered in order to illustrate the computational effort without the influence of the fact that higher codes rates involve higher information throughput.

The coded throughput of the original unpruned algorithm (ref), decreases as the code rate increases. Indeed, frozen bit leaf nodes are faster to process than information bit leaf nodes, in which a threshold detection is necessary. As there are more R0 and REP nodes in low code rates, their pruning is more efficient in the case of low code rates. The same explanation can be given for R1 nodes in high code rates. R1 node pruning is more efficient than R0 node pruning on average. Indeed, a higher amount of computations is saved in R1 nodes than in R0 nodes.

It has also been observed in [10] that when the SPC node size is not limited to 4, the decoding performance may be degraded. Consequently the size is limited to 4 in SPC4. In SPC4+ nodes, there is no size limit. The two node types are considered in Fig. 4. Therefore, the depth at which dedicated

nodes are activated in the proposed decoder can be adjusted, in order to offer a tradeoff between throughput and decoding performance.

According to our experiments, the aforementioned statement about performance degradation caused by SPC4+ nodes is not always accurate depending on the code and decoder parameters. The impact of switching *on* or *off* SPC4+ nodes on decoding performance and throughput at a FER of  $10^{-5}$  is detailed in Fig. 5. It shows that SPC4+ nodes have only a small effect on the decoding performance. With  $L = 8$ , an SNR degradation lower than 0.1 dB is observed, except for one particular configuration. Throughput improvements of 8 to 23 percents are observed. If  $L = 32$ , the SNR losses are more substantial (up to 0.5 dB), whereas throughput improvements are approximately the same. Besides this observation, Fig. 5 shows how the proposed decoder flexibility in the AFF3CT environment enables to optimize easily the decoder tree pruning, both for software implementations or for hardware implementations in which tree pruning can also be applied [28].

### 3.2.3 LLR Quantization

Another important parameter in both software and hardware implementations is the quantization of data in the decoder. More specifically, the quantization of LLRs and partial sums in the decoder have an impact on decoding performance. Quantized implementations of the SC algorithm have already been proposed in [29] but to the best of our knowledge, the proposed decoder is the first software SCL implementation that can benefit from the 8-bit and 16-bit fixed-point representations of LLRs and internal path metrics. In the 8-bit mode LLRs and path metrics are saturated between  $-127$  and  $+127$  after each operation. Moreover, to avoid overflows, the path metrics are normalized after each *update\_paths()* call (cf. Alg. 1) by subtracting the smallest metric to each one of them. Figure 6a shows the BER

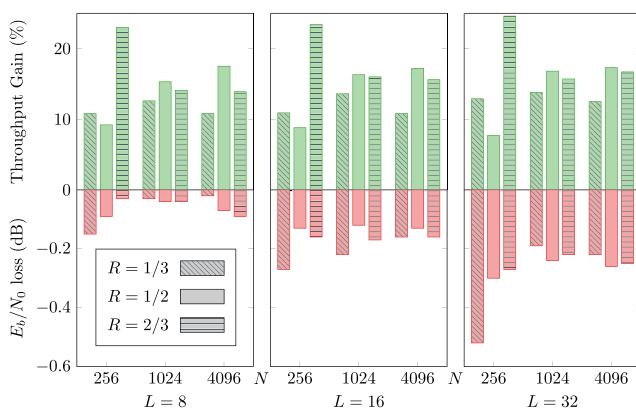


**Figure 5** Effects of using the SPC4+ nodes on the CA-SSCL @  $10^{-5}$  FER compared to a reference where they are not used.

and FER performances of the CA-SSCL decoder for 32-bit floating-point, 16-bit and 8-bit fixed-point representations. One can observe that the REP nodes degrade the decoding performance in a 8-bit representation because of accumulation (red triangles curve). Indeed, it is necessary to add all the LLRs of a REP node together in order to process it, which may lead to an overflow in the case of fixed-point representation. It can happen when the size of the repetition nodes is not limited (REP<sub>2+</sub>). However, the size limitation of the repetition nodes to 8 (REP<sub>8-</sub>) fixes this issue. In Table 2, maximum latency ( $\mathcal{L}_{worst}$  in  $\mu s$ ), average latency ( $\mathcal{L}_{avg}$  in  $\mu s$ ) and information throughput ( $\mathcal{T}_i$  in Mb/s) are given. Note that in 8-bit configuration only the REP<sub>8-</sub> nodes are used. The fixed-point implementation reduces, on average, the latency. In the high SNR region, the frame errors are less frequent. Therefore, the SCL algorithm is less necessary than in low SNR regions for Adaptive SCL algorithms. As the gain of fixed-point implementation benefits more to the SC algorithm than to the SCL algorithm, the throughput is higher in high SNR regions. For instance, up to 425.9 Mb/s is achieved in 8-bit representation with the FA-SSCL decoder. Note that the improvements described in Section 4 are applied to the decoders that are given in Table 2.

### 3.2.4 Supporting Different Variants of the Decoding Algorithms

Besides the  $L$  values, the tree pruning and quantization aspects, the proposed software polar decoder supports different variants of the SCL algorithm: CA-SSCL, PA-SSCL, FA-SSCL.

As shown in [10], the adaptive version of the SCL algorithm yields significant speedups, specially for high SNR. The original adaptive SCL described in [19], denoted

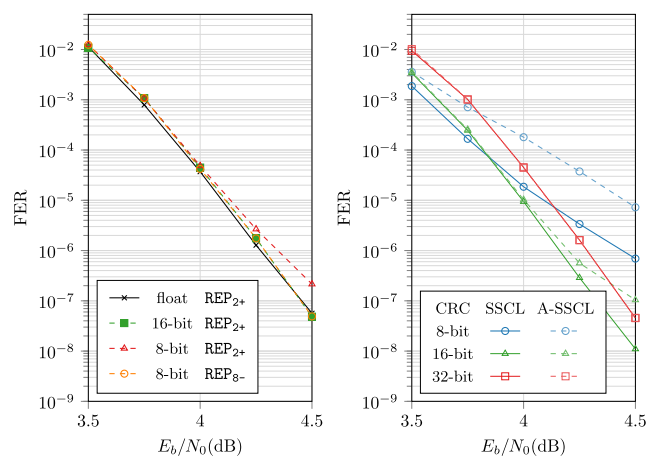


**Figure 6** Decoding performance of the SSCL and the A-SSCL decoders. Code (2048,1723),  $L = 32$ .

**Table 2** Throughput and latency comparisons between floating-point (32-bit) and fixed-point (16-bit and 8-bit) Adaptive SSCL decoders.

Decoder	Prec.	$\mathcal{L}_{worst}$	3.5 dB		4.0 dB		4.5 dB	
			$\mathcal{L}_{avg}$	$\mathcal{T}_i$	$\mathcal{L}_{avg}$	$\mathcal{T}_i$	$\mathcal{L}_{avg}$	$\mathcal{T}_i$
PA-SSCL	32-bit	635	232.3	7.6	41.7	42.1	7.4	237.6
	16-bit	622	219.6	8.0	40.1	43.8	6.6	267.5
	8-bit	651	232.4	7.6	41.2	42.6	6.5	268.3
FA-SSCL	32-bit	1201	67.2	26.1	8.5	207.8	5.1	345.5
	16-bit	1198	68.7	25.6	7.7	225.7	4.3	408.7
	8-bit	1259	71.8	24.4	7.7	227.3	4.1	425.9

Code (2048,1723),  $L = 32$  and 32-bit CRC (GZip)

as Fully Adaptive SCL (FA-SSCL) in this paper, gradually doubles the list depth  $L$  of the SCL decoder when the CRC is not valid for any of the generated codewords at a given stage until the value  $L_{max}$ . By contrast, the adaptive decoding algorithm implemented in [10], called in this paper Partially Adaptive SCL (PA-SSCL), directly increases the list depth from 1 (SC) to  $L_{max}$ . In Fig. 7, the two versions (FA-SSCL and PA-SSCL) are compared on a (2048,1723) polar code and 32-bit CRC (GZip). The LLRs values are based on a 32-bit floating point representation. Note that as the FER performance of PA-SSCL and FA-SSCL are exactly the same, the related error performance plots completely overlap. The throughput of the FA-SSCL algorithm is higher than that of the PA-SSCL algorithm for some SNR values, depending on the code parameters. Considering typical FER values for wireless communication standards ( $10^{-3}$  to  $10^{-5}$ ), in the case of a (2048,1723) polar code, the throughput of FA-SSCL is double that of PA-SSCL with  $L = 8$ , while it is multiplied by a factor of 7 with  $L = 32$ . The drawback of FA-SSCL is that although the average latency decreases, the worst case latency increases.

The adaptive versions of the algorithm achieve better throughputs, but CA-SCL may also be chosen depending on the CRC. One may observe in Fig. 6b that an adaptive decoder dedicated to an 8-bit CRC with a (2048,1723) polar code and  $L = 32$  leads to a loss of 0.5 dB for a FER of  $10^{-5}$  compared to its non adaptive counterpart.

Both polar code genericity and decoding algorithm flexibility are helpful to support the recommendations of wireless communications in an SDR or cloud RAN context. The code and decoder parameters can be dynamically changed in the proposed decoder, while maintaining competitive throughput and latency. The following section introduces algorithmic and implementation-related improvements applied in the proposed decoders to keep a low decoding time.

## 4 Software Implementation Optimizations

The genericity and flexibility of the formerly described decoder prevent from using some optimizations. Unrolling the description as in [10] is not possible at runtime, although code generation could be used to produce an unrolled version of any decoder as in [30]. Moreover, in the case of large code lengths, the unrolling strategy can generate very large compiled binary files. This can cause instruction cache misses that would dramatically impact the decoder throughput. By contrast, the size of the executable files of the proposed decoder is constant with respect to the code parameters ( $N, L, K$ ). In the experiments reported in this paper, code size was not a significant issue as the number of cycles lost to cache misses is less than 0.01% of the total number of cycles. Still, some implementation improvements are necessary in order to be competitive with specific unrolled decoders of the literature. The software library for polar codes from [30, 31] enables the proposed

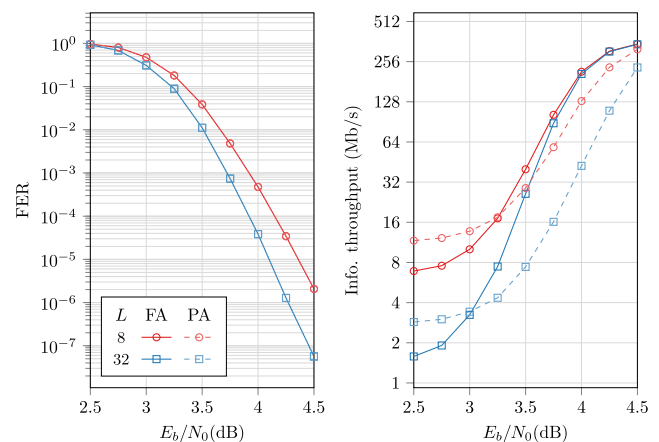


**Figure 7** Frame Error Rate (FER) performance and throughput of the FA-SSCL and PA-SSCL decoders. Code (2048,1723) and 32-bit CRC (GZip). 32-bit floating-point representation.



decoders to benefit from the SIMD instructions for various target architectures. Optimizations of CRC checking benefit to both the non-adaptive and adaptive versions of the CA-SCL algorithms. The new sorting technique presented in Section 4.3 can be applied to each variation of the SCL algorithm. Finally, an efficient implementation of the partial sums memory management is proposed. It is particularly effective for short polar codes.

#### 4.1 Polar Application Programming Interface

Reducing the decoding time with SIMD instructions is a classical technique in former software polar decoder implementations. The proposed list decoders are based on specific building blocks included from the Polar API [30, 31]. These blocks are fast and optimized implementations of the  $f$ ,  $g$ ,  $h$  (and their variants) polar intrinsic functions. Figure 8 details the SIMD implementation of these functions. This implementation is based on MIPP [32], a SIMD wrapper for the intrinsic functions, and the template meta-programming technique. Consequently, the description is clear, portable, multi-format (32-bit floating-point, 16-bit and 8-bit fixed-points) and as fast as an architecture specific code. The `mipp::Reg<B>` and `mipp::Reg<R>` types correspond to SIMD registers. B and R define the type of the elements that are contained in this register. B for *bit* could be `int`, `short` or `char`. R for *real* could be `float`, `short` or `char`. In Fig. 8, each operation is made on multiple elements at the same time. For

```

1 class API_polar
2 {
3   template <typename R>
4   mipp::Reg<R> f_simd(const mipp::Reg<R> &la,
5                     const mipp::Reg<R> &lb)
6   {
7     auto abs_la = mipp::abs(la);
8     auto abs_lb = mipp::abs(lb);
9     auto abs_min = mipp::min(abs_la, abs_lb);
10    auto sign = mipp::sign(la, lb);
11    auto lc = mipp::neg(abs_min, sign);
12
13    return lc;
14  }
15
16  template <typename B, typename R>
17  mipp::Reg<R> g_simd(const mipp::Reg<R> &la,
18                    const mipp::Reg<R> &lb,
19                    const mipp::Reg<B> &sa)
20  {
21    auto neg_la = mipp::neg(la, sa);
22    auto lc = neg_la + lb;
23
24    return lc;
25  }
26
27  template <typename B>
28  mipp::Reg<B> h_simd(const mipp::Reg<B> &sa,
29                    const mipp::Reg<B> &sb)
30  {
31    return sa ^ sb;
32  }
33 };

```

**Figure 8** C++ SIMD implementation of the  $f$ ,  $g$  and  $h$  functions.

instance, line 22, the addition between all the elements of the `neg_la` and `lb` registers is executed in one CPU cycle.

In the context of software decoders, there are two well-known strategies to exploit SIMD instructions: use the elements of a register to compute 1) many frames in parallel (INTER frame) or 2) multiple elements from a single frame (INTRA frame). In this paper, only the INTRA frame strategy is considered. The advantage of this strategy is the latency reduction by comparison to the INTER frame strategy. However, due to the nature of the polar codes, there are sometimes not enough elements to fill the SIMD registers completely. This is especially true in the nodes near the leaves. For this reason, SIMD instructions in the lower layers of the tree do not bring any speedup. In this context, the building blocks of the Polar API automatically switch from SIMD to sequential implementations. In the case of the CA-SSCL algorithm, using SIMD instructions for decoding a (2048,1723) polar code leads to an improvement of 20% of the decoding throughput on average for different values of the list depth  $L$ .

#### 4.2 Improving Cyclic Redundancy Checking

By profiling the Adaptive SCL decoder, one may observe that a significant amount of time is spent to process the cyclic redundancy checks. Its computational complexity is  $O(LN)$  versus the computational complexity of the SCL decoding,  $O(LN \log N)$ . The first is not negligible compared to the second.

In the adaptive decoder, the CRC verification is performed a first time after the SC decoding. In the following, we show how to reduce the computational complexity of these CRC verifications.

First, an efficient CRC checking code has been implemented. Whenever the decoder needs to check the CRC, the bits are packed and then computed 32 by 32. In order to further speed up the implementation, a lookup table is used to store pre-computed CRC sub-sequences, and thus reading CRC values directly from this table reduces the computational complexity. The size of the lookup table is 1 KB.

After a regular SC decoding, a decision vector of size  $N$  is produced. Then, the  $K$  information bits must be extracted to apply cyclic redundancy check. The profiling of our decoder description shows that this extraction takes a significant amount of time compared to the check operation itself. Consequently, a specific extraction function was implemented. This function takes advantage of the leaf node type knowledge to perform efficient multi-element copies.

Concerning SCL decoding, it is possible to sort the candidates according to their respective metrics and then to check the CRC of each candidate from the best to the worst. Once a candidate with a valid CRC is found, it is chosen

as the decision. This method is strictly equivalent to do the cyclic redundancy check of each candidate and then to select the one with the best metric. With the adopted order, decoding time is saved by reducing the average number of checked candidates.

### 4.3 LLR and Metric Sorting

Metric sorting is involved in the aforementioned path selection step, but also in the *update\_paths()* sub-routine (Alg. 1, 1.16) and consequently in each leaf. Sorting the LLRs is also necessary in R1 and SPC nodes. Because of a lack of information about the sorting technique presented in [10], its reproduction is not possible. In the following of the paragraph the sorting algorithm used in the SCL decoder is described.

In R1 nodes, a Chase-2 [33] algorithm is applied. The two minimum absolute values of the LLRs have to be identified. The way to do the minimum number of comparisons to identify the 2 smallest (or the two largest) of  $n \geq 2$  elements was originally described by Schreier in [12] and reported in [34]. The lower stages of this algorithm can be parallelized thanks to SIMD instructions in the way described in [35]. According to our experimentations, Schreier’s algorithm is the most efficient compared to parallelized Batchner’s merge exchange, partial quick-sort or heap-sort implemented in the C++ standard library in the case of R1 nodes.

Concerning path metrics, partial quick-sort appeared to yield no gains in terms of throughput by comparison with the algorithm in [12], neither did heap-sort or parallelized Batchner’s merge exchange. For a matter of consistency, only Schreier’s algorithm is used in the proposed decoder, for both LLR sorting in R1 and SPC nodes and for path metrics sorting. The sorting of path metrics is applied to choose the paths to be removed, kept or duplicated.

### 4.4 Partial Sum Memory Management

An SCL decoder can be seen as  $L$  replications of an SC decoder. The first possible memory layout is the one given in Fig. 1. In this layout, the partial sums  $\hat{s}$  of each node is stored in a dedicated array. Therefore, a memory of size  $2N - 1$  bits is necessary in the SC decoder, or  $L(2N - 1)$  bits in the SCL decoder. This memory layout is described in [2] and applied in previous software implementations [10, 11, 36].

A possible improvement is to change the memory layout to reduce its footprint. Due to the order of operations in both SC and SCL algorithms, the partial sums on a given layer are only used once by the  $h$  function and can then be overwritten. Thus, a dedicated memory allocation is not necessary at each layer of the tree. The memory can be

shared between the stages. Therefore the memory footprint can be reduced from  $2N - 1$  to  $N$  in the SC decoder as shown in [37]. A reduction from  $L(2N - 1)$  to  $LN$  can be obtained in the SCL decoder.

In the case of the SCL algorithm,  $L$  paths have to be assigned to  $L$  partial sum memory arrays. In [2], this assignment is made with pointers. The advantage of pointers is that when a path is duplicated, in the *update\_paths()* sub-routine of Alg. 1, the partial sums are not copied. Actually, they can be shared between paths thanks to the use of pointers. This method limits the number of memory transactions. Unfortunately, it is not possible to take advantage of the memory space reduction: the partial sums have to be stored on  $L(2N - 1)$  bits. There is an alternative to this mechanism. If a logical path is statically assigned to a memory array, no pointers are necessary at the cost that partial sums must be copied when a path is duplicated (only  $LN$  bits are required). This method is called  $SSCL_{cpy}$  whereas the former is called  $SSCL_{ptr}$ .

Our experiments have proved that the overhead of handling pointers plus the extra memory space requirement cause the  $SSCL_{cpy}$  to be more efficient than the  $SSCL_{ptr}$  for short and medium code lengths, as shown in Fig. 9. The 32-bit version uses floating-point LLRs, whereas 16-bit and 8-bit versions are in fixed-point. Notice that in this work, each bit of the partial sums is stored on an 8-bit, 16-bit or 32-bit number accordingly to the LLR data type. The code rate  $R$  is equal to  $1/2$ . The throughput of the  $SSCL_{cpy}$  version is higher for  $N \leq 8192$  whereas the  $SSCL_{ptr}$  version is more efficient for higher values of  $N$ . Although it does not appear in Fig. 9, experiments showed that the lower  $L$  is, the more efficient  $SSCL_{cpy}$  is compared to  $SSCL_{ptr}$ . Figure 9 also illustrates the impact of the representation of partial sums. For very high values of  $N$ , 8-bit fixed point representation takes advantage of fewer cache misses. According to the results presented in Fig. 2, as the decoding performance improvements of the SCL algorithm are not

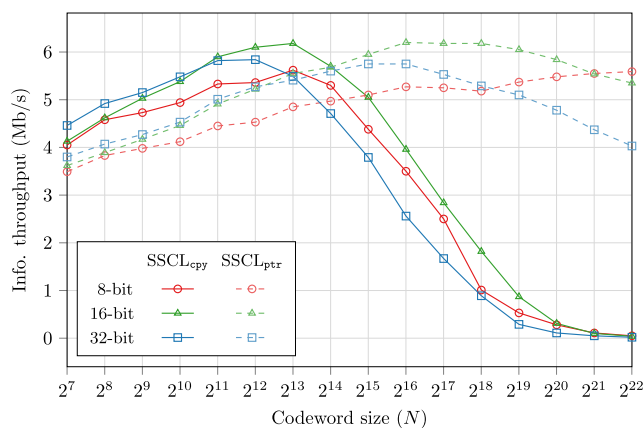


Figure 9 Information throughput of the SSCL decoder depending on  $N$  and the partial sums management.  $R = 1/2$ ,  $L = 8$ .

very significant compared to the SC algorithm for long polar codes, SSCL<sub>cpy</sub> is the appropriate solution in most practical cases.

In our decoder description, LLRs are managed with pointers, as it is the case in other software implementations of the literature [10, 11, 36]. We tried to remove the pointer handling as for the partial sums, but it appeared that it was not beneficial in any use case.

### 4.5 Memory Footprint

The exact memory footprint of the decoders is hard to obtain as there are many small buffers related to the implementation. However, the memory footprint is mainly driven by the LLRs ( $\lambda$ ) and the partial sums ( $\hat{s}$ ) as they linearly depend on  $LN$ . The buffers related to the path metrics can be neglected as they linearly depend on  $L$ . The memory footprint of the CRC is also negligible as the only requirement is a lookup table of 256 integers. Table 3 summarizes the memory footprint estimation of the various decoders.  $Q$  stands for the size of the element (1, 2 or 4 bytes). The channel LLRs are taken into account in the approximation. As explained in the previous section, the SSCL<sub>ptr</sub> version of the code requires twice the amount of data for the partial sums. Notice that the memory footprint of the adaptive decoders is slightly higher than the other SCL since it includes an additional SC decoder.

## 5 Experiments and Measurements

Throughput and latency measurements are detailed in this section. The proposed decoder implementation is compared with the previous software decoders. Despite the additional levels of genericity and flexibility, the proposed implementation is very competitive with its counterparts. Note that all the results presented in the following can be reproduced with the AFF3CT tool.

During our investigations, all the throughput and latency measurements have been obtained on a single core of an Intel i5-6600K CPU (Skylake architecture with AVX2 SIMD) with a base clock frequency of 3.6 GHz and a maximum turbo frequency of 3.9 GHz. The description has been compiled on Linux with the C++ GNU compiler

**Table 3** Polar decoders data memory footprint (in bytes).

Algorithms	Memory Footprint
(CA-)SSCL <sub>cpy</sub>	$\mathcal{O}((2L + 1)NQ)$
(CA-)SSCL <sub>ptr</sub>	$\mathcal{O}((3L + 1)NQ)$
A-SSCL <sub>cpy</sub>	$\mathcal{O}((2L + 3)NQ)$
A-SSCL <sub>ptr</sub>	$\mathcal{O}((3L + 3)NQ)$

(version 5.4.0) and with the following options: `-Ofast -march=native -funroll-loops`.

### 5.1 Fully Adaptive SCL

Being able to easily change the list size of the SCL decoders enables the use of the FA-SSCL algorithm. With an unrolled decoder as proposed in [10], the fully adaptive decoder would imply to generate a fully unrolled decoder for each value of the list depth. In our work, only one source code gives the designer the possibility to run each variation of the SCL decoders. Using the FA-SSCL algorithm is the key to achieve the highest possible throughput. As shown in Table 2, with an 8-bit fixed point representation of the decoder inner values, the achieved throughput in the case of the (2048,1723) polar code is about 425 Mb/s on the i5-6600K for an  $E_b/N_0$  value of 4.5 dB. It corresponds to a FER of  $5 \times 10^{-8}$ . This throughput is almost 2 times higher than the throughput of the PA-SSCL algorithm. The highest throughput increase from PA-SSCL to FA-SSCL, of about 380%, is in the domain where the FER is between  $10^{-3}$  and  $10^{-5}$ . It is the targeted domain for wireless communications like LTE or 5G. In these conditions, the throughput of FA-SSCL algorithm is about 227 Mb/s compared to 42 Mb/s for the PA-SSCL algorithm.

In Adaptive SCL algorithms, the worst case latency is the sum of the latency of each triggered algorithm. In the case of PA-SSCL with  $L_{max} = 32$ , it is just the sum of the latency of the SC algorithm, plus the latency of the SCL algorithm with  $L = 32$ . In the case of the FA-SSCL algorithm, it is the sum of the decoding latency of the SC algorithm and all the decoding latencies of the SCL algorithm for  $L = 2, 4, 8, 16, 32$ . This is the reason why the worst latency of the PA-SSCL algorithm is lower while the average latency and consequently the average throughput is better with the FA-SSCL algorithm.

### 5.2 Comparison with State-of-the-Art SCL Decoders

The throughput and latency of the proposed decoder compared to other reported implementations are detailed in Table 4. For all the decoders, all the available tree pruning optimizations are applied excluding the SPC4+ nodes because of the error performance degradation they induce. Each decoder is based on a 32-bit floating-point representation. The polar code parameters are  $N = 2048$ ,  $K = 1723$  and the 32-bit GZip CRC is used. The list size is  $L = 32$ .

The latency given in Table 4 is the worst case latency and the throughput is the average information throughput. The first version, CA-SCL, is the implementation of the CA-SCL algorithm without any tree pruning. As mentioned before the throughput of the proposed CA-SSCL decoder

**Table 4** Throughput and latency comparison with state-of-the-art SCL decoders.

Target	Decoder	$\mathcal{L}_{worst}$ ( $\mu s$ )	$\mathcal{T}_i$ (Mb/s)		
			3.5 dB	4.0 dB	4.5 dB
i7-4790K	CA-SCL [36]	1572	1.10	1.10	1.10
i7-2600	CA-SCL [11]	23000	0.07	0.07	0.07
	CA-SSCL[11]	3300	0.52	0.52	0.52
	PA-SSCL [11]	$\approx 3300$	0.9	4.90	54.0
i7-2600	CA-SCL [10]	2294	0.76	0.76	0.76
	CA-SSCL[10]	433	4.0	4.0	4.0
	PA-SSCL [10]	$\approx 433$	8.6	33.0	196.0
i7-2600	This CA-SCL	4819	0.37	0.37	0.37
	This CA-SSCL	770	2.3	2.3	2.3
	This PA-SSCL	847	5.5	31.1	168.4
	This FA-SSCL	1602	19.4	149.0	244.3
i5-6600K	This CA-SCL	3635	0.48	0.48	0.48
	This CA-SSCL	577	3.0	3.0	3.0
	This PA-SSCL	635	7.6	42.1	237.6
	This FA-SSCL	1201	26.1	207.8	345.5

32-bit floating-point representation. Code (2048,1723),  $L = 32$ , 32-bit CRC

(2.3 Mb/s) is only halved compared to the specific unrolled CA-SSCL decoder described in [10] (4.0 Mb/s). The proposed CA-SSCL decoder is approximately 4 times faster than the generic implementation in [11] (0.52 Mb/s) and 2 times faster than the CA-SCL implementation in [36] (1.1 Mb/s) thanks to the implementation improvements detailed in Section 4. Furthermore, the proposed decoder exhibits a much deeper level of genericity and flexibility than the ones proposed in [11, 36]. Indeed, in these previous works, the following features were not enabled: the customization of the tree pruning, the 8-bit and 16-bit fixed-point representations of the LLRs, the puncturing patterns and the FA-SSCL algorithm.

When implemented on the same target (i7-2600), the proposed PA-SSCL is competitive with the unrolled PA-SSCL in [10], being only two times slower. This can be explained by the improvements concerning the CRC that are described in Section 4.2, especially the information bits extraction in the SC decoder. Finally, as mentioned before, the throughput of the proposed FA-SSCL significantly outperforms all the other SCL decoders (up to 345.5 Mb/s at 4.5 dB in 32-bit floating-point).

## 6 Conclusion

The trend towards Cloud RAN networks in the context of mobile communications and the upcoming 5G standard

motivated an investigation of the possibility of implementing generic and flexible software polar decoders. Means of implementing such flexible decoders are reported in this paper. A single source code is necessary to address any code lengths, code rates, frozen bits sets, puncturing patterns and cyclic redundancy check polynomials.

This genericity is obtained without sacrificing the throughput of the decoders, thanks to the possibility to adjust the decoding algorithm and the possibility to apply multiple implementation related and algorithmic optimizations. In fact, to the best of our knowledge, the proposed adaptive SCL decoder is the fastest to be found in the literature, with a throughput of 425 Mb/s on a single core for  $N = 2048$  and  $K = 1723$  at 4.5 dB.

The reported decoder being included in the open-source AFF3CT tool, all the results presented in this paper can be easily reproduced. Moreover, this tool can be used for polar codes exploration, which is of interest for the definition of digital communication standards and for practical implementations in an SDR environment.

**Acknowledgements** The authors would like to thank the Natural Sciences and Engineering Research Council of Canada, Prompt, and Huawei Technologies Canada Co. Ltd. for financial support to this project. This work was also supported by a grant overseen by the French National Research Agency (ANR), ANR-15-CE25-0006-01.

**Publisher's Note** Springer Nature remains neutral with regard to jurisdictional claims in published maps and institutional affiliations.

## References

1. Arikan, E. (2009). Channel polarization: a method for constructing capacity-achieving codes for symmetric binary-input memoryless channels. *IEEE Transactions on Information Theory (TIT)*, 55(7), 3051–3073.
2. Tal, I., & Vardy, A. (2011). List decoding of polar codes. In *Proceedings of the IEEE International Symposium on Information Theory (ISIT)* (pp. 1–5).
3. “3GPP TSG RAN WG1 meeting #87, Chairman’s notes of agenda item 7.1.5 Channel coding and modulation,” 2016.
4. Wübben, D., Rost, P., Bartelt, J.S., Lalam, M., Savin, V., Gorgoglione, M., Dekorsy, A., Fettweis, G. (2014). Benefits and impact of cloud computing on 5G signal processing: flexible centralization through cloud-ran. *IEEE Signal Processing Magazine*, 31(6), 35–44.
5. Rost, P., Bernardos, C.J., De Domenico, A., Di Girolamo, M., Lalam, M., Maeder, A., Sabella, D., Wübben, D. (2014). Cloud technologies for flexible 5G radio access networks. *IEEE Communications Magazine*, 52(5), 68–76.
6. Ericsson (2015). Cloud ran - the benefits of virtualization, centralisation and coordination, Tech. Rep. [Online]. Available: <https://www.ericsson.com/assets/local/publications/white-papers/wp-cloud-ran.pdf>.
7. Huawei (2013). 5G: A technology vision, Tech. Rep. [Online]. Available: [https://www.huawei.com/ilink/en/download/HW\\_314849](https://www.huawei.com/ilink/en/download/HW_314849).
8. Rodriguez, V.Q., & Guillemin, F. (2017). Towards the deployment of a fully centralized cloud-ran architecture. In *Proceedings of the IEEE International Wireless Communications and Mobile Computing Conference (IWCMC)* (pp. 1055–1060).
9. Nikaein, N. (2015). Processing radio access network functions in the cloud: critical issues and modeling. In *Proceedings of the ACM International Workshop on Mobile Cloud Computing and Services (MCS)* (pp. 36–43).
10. Sarkis, G., Giard, P., Vardy, A., Thibeault, C., Gross, W.J. (2016). Fast list decoders for polar codes. *IEEE Journal on Selected Areas in Communications (JSAC)*, 34(2), 318–328.
11. Sarkis, G., Giard, P., Vardy, A., Thibeault, C., Gross, W.J. (2014). Increasing the speed of polar list decoders. In *Proceedings of the IEEE International Workshop on Signal Processing Systems (SiPS)* (pp. 1–6).
12. Schreier, J. (1932). On tournament elimination systems. *Mathesis Polska*, 7, 154–160.
13. Tal, I., & Vardy, A. (2013). How to construct polar codes. *IEEE Transactions on Information Theory (TIT)*, 59(10), 6562–6582.
14. Trifonov, P. (2012). Efficient design and decoding of polar codes. *IEEE Transactions on Communications*, 60(11), 3221–3227.
15. Le Gal, B., Leroux, C., Jego, C. (2015). Multi-Gb/s software decoding of polar codes. *IEEE Transactions on Signal Processing (TSP)*, 63(2), 349–359.
16. Sarkis, G., Giard, P., Vardy, A., Thibeault, C., Gross, W.J. (2014). Fast polar decoders: algorithm and implementation. *IEEE Journal on Selected Areas in Communications (JSAC)*, 32(5), 946–957.
17. Balatsoukas-Stimming, A., Parizi, M.B., Burg, A. (2015). LLR-Based successive cancellation list decoding of polar codes. *IEEE Transactions on Signal Processing (TSP)*, 63(19), 5165–5179.
18. Alamdar-Yazdi, A., & Kschischang, F. (2011). A simplified successive-cancellation decoder for polar codes. *IEEE Communications Letters*, 15(12), 1378–1380.
19. Li, B., Shen, H., Tse, D. (2012). An adaptive successive cancellation list decoder for polar codes with cyclic redundancy check. *IEEE Communications Letters*, 16(12), 2044–2047.
20. Matsumoto, M., & Nishimura, T. (1998). Mersenne twister: a 623-dimensionally equidistributed uniform pseudo-random number generator. *ACM Transactions on Modeling and Computer Simulation (TOMACS)*, 8(1), 3–30.
21. Box, G.E.P., Muller, M.E., et al. (1958). A note on the generation of random normal deviates. *The Annals of Mathematical Statistics*, 29(2), 610–611.
22. Dahlman, E., Parkvall, S., Skold, J. (2013). *4G: LTE/LTE-advanced for mobile broadband*. New York: Academic Press.
23. Wang, R., & Liu, R. (2014). A novel puncturing scheme for polar codes. *IEEE Communications Letters*, 18(12), 2081–2084.
24. Niu, K., Chen, K., Lin, J.R. (2013). Beyond turbo codes: rate-compatible punctured polar codes. In *Proceedings of the IEEE International Conference on Communications (ICC)* (pp. 3423–3427).
25. Miloslavskaya, V. (2015). Shortened polar codes. *IEEE Transactions on Information Theory (TIT)*, 61(9), 4852–4865.
26. “Cyclic redundancy check,” [https://en.wikipedia.org/wiki/Cyclic\\_redundancy\\_check](https://en.wikipedia.org/wiki/Cyclic_redundancy_check), accessed: 2017-03-13.
27. Zhang, Q., Liu, A., Pan, X., Pan, K. (2017). CRC Code design for list decoding of polar codes. *IEEE Communications Letters*, 21(6), 1229–1232.
28. Lin, J., Xiong, C., Yan, Z. (2014). A reduced latency list decoding algorithm for polar codes. In *Proceedings of the IEEE International Workshop on Signal Processing Systems (SiPS)* (pp. 1–6).
29. Giard, P., Sarkis, G., Leroux, C., Thibeault, C., Gross, W.J. (2016). Low-latency software polar decoders. *Springer Journal of Signal Processing Systems (JSPS)*, 90, 31–53.
30. Cassagne, A., Le Gal, B., Leroux, C., Aumage, O., Barthou, D. (2015). An efficient, portable and generic library for successive cancellation decoding of polar codes. In *Proceedings of the Springer International Workshop on Languages and Compilers for Parallel Computing (LCPC)* (pp. 303–317).
31. Cassagne, A., Aumage, O., Leroux, C., Barthou, D., Le Gal, B. (2016). Energy consumption analysis of software polar decoders on low power processors. In *Proceedings of the IEEE European Signal Processing Conference (EUSIPCO)* (pp. 642–646).
32. Cassagne, A., Aumage, O., Barthou, D., Leroux, C., Jégo, C. (2018). MIPP: A portable c++ simd wrapper and its use for error correction coding in 5G standard. In *Proceedings of the 2018 4th Workshop on Programming Models for SIMD/vector Processing: ACM*.
33. Chase, D. (1972). Class of algorithms for decoding block codes with channel measurement information. *IEEE Transactions on Information Theory (TIT)*, 18(1), 170–182.
34. Knuth, D. (1973). *The art of computer programming*. Reading: Addison-Wesley. no. 3.
35. Furtak, T., Amaral, J.N., Niewiadomski, R. (2007). Using SIMD registers and instructions to enable instruction-level parallelism in sorting algorithms. In *Proceedings of the ACM Symposium on Parallel Algorithms and Architectures* (pp. 348–357).
36. Shen, Y., Zhang, C., Yang, J., Zhang, S., You, X. (2016). Low-latency software successive cancellation list polar decoder using stage-located copy. In *Proceedings of the IEEE International Conference on Digital Signal Processing (DSP)*.
37. Leroux, C., Raymond, A.J., Sarkis, G., Gross, W.J. (2013). A semi-parallel successive-cancellation decoder for polar codes. *IEEE Transactions on Signal Processing (TSP)*, 61(2), 289–299.



**Mathieu Léonardon** received the M.Sc. degree from Bordeaux INP, Bordeaux, France, in 2015. He received the Ph.D. in electronics engineering from Polytechnique Montréal, Canada, and from the University of Bordeaux, France, in 2018. His research is focused on error-correcting codes, flexible hardware architectures, and software implementations of signal processing algorithms.



**Adrien Cassagne** received the M.Sc. degree in computer science from the University of Bordeaux, France, in 2013. He is currently working toward the Ph.D. degree at the University of Bordeaux. His research interests are in the design of efficient and flexible software implementations for modern decoding error-correcting codes such as LDPC, turbo and polar codes. More precisely, he looks at different aspects of parallelism such as multi-node, multi-threading or vectorization.



**Camille Leroux** received his M.Sc. degree in Electronics Engineering from the University of South Brittany, Lorient, France, in 2005. He received his Ph.D. degree in Electronics Engineering from TELECOM Bretagne, Brest, France, in 2008. From 2008 to 2011 he worked as a Post Doctoral Research Associate in the Electrical and Computer Engineering Department at McGill University, Montreal, QC, Canada. He is an Associate Professor at Bordeaux INP since 2011. He was also a visiting student in the Electrical and Computer Engineering Department at Aalborg University, Denmark, in 2004 and at University of Alberta, AB, Canada, in 2005. His research interests encompass algorithmic and architectural aspects of channel decoder implementation. More generally, he is interested in the hardware and software implementation of computationally intensive algorithms in a real-time environment.

deux INP since 2011. He was also a visiting student in the Electrical and Computer Engineering Department at Aalborg University, Denmark, in 2004 and at University of Alberta, AB, Canada, in 2005. His research interests encompass algorithmic and architectural aspects of channel decoder implementation. More generally, he is interested in the hardware and software implementation of computationally intensive algorithms in a real-time environment.



**Christophe Jégo** was born in Auray, France, in 1973. He received the M.S. and Ph.D. degrees from the Université Rennes 1, Rennes, France, in 1996 and 2000, respectively. He joined the Electronic Engineering Department of TELECOM Bretagne, Brest, France, as a full-Time Associate Professor in 2001. He was a visiting professor in the Department of Electrical and Computer Engineering at McGill University, Montreal, Quebec, Canada, during 10 months

(Sept. 2006–June 2007). In 2009, he received Research Habilitation from University of Bretagne Sud, Lorient, France. It is the highest French university diploma passed after a few years of active research and student supervision. He joined the graduate engineering school ENSEIRB-MATMECA, Bordeaux, France, as a full-Time Professor in 2010. Currently, he is member of the CNRS IMS laboratory, UMR 5218. His research activities are concerned with analysis and design of architectures for iterative processing in the digital communication systems.



**Louis-Philippe Hamelin** received his B.Eng. degree in computer engineering from McGill University, Montreal, Canada, in 1999. Between 2000 and 2013, he worked as an ASIC design engineer/lead focusing on design and implementation of chipsets targeting various telecommunication protocols and applications. In 2013, he joined Huawei Technologies as an ASIC researcher for 5G wireless applications. His work interest focuses on efficient algorithm implementation in hardware and low power design. As a technical expert on Polar Decoder architectures and implementations, he participated in 3GPP discussions and contributed to the adoption of the Polar code for 5G/NR Uplink/Downlink control channel for eMBB.

As a technical expert on Polar Decoder architectures and implementations, he participated in 3GPP discussions and contributed to the adoption of the Polar code for 5G/NR Uplink/Downlink control channel for eMBB.



**Yvon Savaria** (S'77–M'86–SM'97–F'08) received the B.Eng. and M.Sc.A. degrees in electrical engineering from Polytechnique Montréal, Canada, in 1980 and 1982, respectively. He received the Ph.D. in electrical engineering in 1985 from McGill University, Canada.

Since 1985, he has been with Polytechnique Montréal, where he is currently Professor. He has carried out work in several areas related to microelectronic circuits and

Microsystems such as testing, verification, validation, clocking methods, defect and fault tolerance, effects of radiation on electronics, high-speed interconnects and circuit design techniques, CAD methods, reconfigurable computing and applications of microelectronics to telecommunications, aerospace, image processing, video processing, radar signal processing, and digital signal processing acceleration. He is currently involved in several projects that relate to aircraft embedded systems, green IT, wireless sensor network, virtual network, computational efficiency and application specific architecture design. He holds 16 patents, has published 140 journal papers and 440 conference papers, and was the thesis advisor of 150 graduate students who completed their studies.

Dr. Savaria has been working as a consultant or was sponsored for carrying research by Bombardier, CNRC, Design Workshop, Dolphin, DREO, Genesis, Gennum, Hyperchip, ISR, LTRIM, Miranda, MiroTech, Nortel, Octasic, PMC-Sierra, Technocap, Thales, Tundra and VXP. He is a member of the Regroupement Stratégique en Microélectronique du Québec (RESMIQ), of the Ordre des Ingénieurs du Québec (OIQ), and was a member of CMC Microsystems board since 1999 and chairman of that board from 2008 to 2010. He was awarded in 2001 a Tier 1 Canada Research Chair ([www.chairs.gc.ca](http://www.chairs.gc.ca)) on design and architectures of advanced microelectronic systems that he held until 2014. He also received in 2006 a Synergy Award of the Natural Sciences and Engineering Research Council of Canada.

## Affiliations

Mathieu Léonardon<sup>1,2</sup>  · Adrien Cassagne<sup>1,3</sup> · Camille Leroux<sup>1</sup> · Christophe Jégo<sup>1</sup> · Louis-Philippe Hamelin<sup>4</sup> · Yvon Savaria<sup>2</sup>

Adrien Cassagne  
adrien.cassagne@ims-bordeaux.fr

Camille Leroux  
camille.leroux@ims-bordeaux.fr

Christophe Jégo  
christophe.jego@ims-bordeaux.fr

Louis-Philippe Hamelin  
louis.hamelin@huawei.com

Yvon Savaria  
yvon.savaria@polymtl.ca

- <sup>1</sup> IMS Laboratory, UMR CNRS 5218, Bordeaux INP, University of Bordeaux, Talence, France
- <sup>2</sup> Polytechnique Montréal, Montréal, QC, Canada
- <sup>3</sup> Inria, Bordeaux Institute of Technology, LaBRI/CNRS, Bordeaux, France
- <sup>4</sup> Huawei Technologies Canada Co. LTD, Ottawa, ON, Canada